Optical second-harmonic scattering from a non-diffusive random distribution of nonlinear domains

Jorge Bravo-Abad,[1,2,5] **Xavier Vidal,**[3] **Jorge L. Domínguez Juárez,**[3] **and Jordi Martorell**[3,4,6]

[1]*Physics Department, Massachusetts Institute of Technology, Cambridge, MA 02139, USA*
[2]*Departamento de Física Teórica de la Materia Condensada, Universidad Autónoma de Madrid, E-28049, Madrid, Spain*
[3]*ICFO–Institut de Ciències Fotòniques, Mediterranean Technology Park, 08860 Castelldefels, Spain*
[4]*Departament de Física i Enginyeria Nuclear, Universitat Politècnica de Catalunya, 08222 Terrassa, Spain*
[5]*jbravo@mit.edu*
[6]*jordi.martorell@icfo.es*

Abstract: We show that the weak second harmonic light generated from a random distribution of nonlinear domains of transparent Strontium Barium Niobate crystals can display a particularly intense generation in the forward direction. By using a theoretical model able to analyze the optical response of arbitrary distributions of three-dimensional nonlinear volumes of any shape, we found that the physical origin of this observation can be explained in terms of the scattering of light by a single nonlinear domain.

OCIS codes: (190.0190) Nonlinear optics; (190.2620) Harmonic generation and mixing; (190.4720) Optical nonlinearities of condensed matter.

References and links

1. R. C. Miller, "Optical harmonic generation in single crystal BaTiO3," Phys. Rev. **134**, A1313–A1319 (1964).
2. C. F. Dewey Jr. and L. O. Hocker, "Enhanced nonlinear optical effects in rotationally twinned crystals," Appl. Phys. Lett. **26**, 442–444 (1975).
3. M. Baudrier-Raybaut, R. Hadar, Ph. Kupecek, Ph. Lemasson, and E. Rosencher, "Random quasi-phase-matching in bulk polycrystalline isotropic nonlinear materials," Nature **432**, 374-376 (2004).
4. X. Vidal and J. Martorell, "Generation of light in media with a random distribution of nonlinear domains," Phys. Rev. Lett. **97**, 013902 (2006).
5. S. Kawai, T. Ogawa, H. S. Lee, R. C. DeMattei, and R. S. Feigelson, "Second-harmonic generation from needle-like ferroelectric domains in Sr0.6Ba0.4Nd2O6 single crystals," Appl. Phys. Lett. **73**, 768–770 (1998).
6. R. Fischer, S. M. Saltiel, D. N. Neshev, W. Krolikowski, and Yu. S. Kivshar, "Broadband femtosecond frequency doubling in random media," Appl. Phys. Lett. **89**, 191105 (2006).
7. J. Trull, C. Cojocaru, R. Fischer, S. M. Saltiel, K. Staliunas, R. Herrero, R. Vilaseca, D. N. Neshev, W. Krolikowski, and Y. S. Kivshar, "Second-harmonic parametric scattering in ferroelectric crystals with disordered nonlinear domain structures," Opt. Express **15**, 15868–15877 (2007).
8. See for instance, A. Ishimaru, *Wave Propagation and Scattering in Random Media* (IEEE Press, New York, 1997).
9. P. D. Maker, R. W. Terhune, M. Nisenhoff, and C. M. Savage, "Effects of dispersion and focusing on the production of optical harmonics," Phys. Rev. Lett. **8**, 21–22 (1962).
10. J.-X. Cheng and X. S. Xie, "Green's function formulation for third-harmonic generation microscopy," J. Opt. Soc. Am. B **19**, 1604–1610 (2002).
11. E. Yew and C. Sheppard, "Effects of axial field components on second harmonic generation microscopy," Opt. Express **14**, 1167–1174 (2006)

#128859 - $15.00 USD Received 24 May 2010; revised 10 Jun 2010; accepted 12 Jun 2010; published 16 Jun 2010

12. See for instance, L. Novotny and B. Hecht, *Principles of Nano-Optics* (Cambridge Univ. Press, Cambridge, 2006), pp. 25–30.
13. R. W. Boyd, *Nonlinear Optics*, 2nd Ed. (Academic, San Diego, 2003), pp. 37–38.
14. D. L. Andrews, P. Allcock, and A. A. Demidov, "Theory of second harmonic generation in randomly oriented species," Chem. Phys. **190**, 1–9 (1995).
15. S. Brasselet, V. Le Floch, F. Treussart, J.-F. Roch, J. Zyss, E. Botzung-Appert, and A. Ibanez, "In situ diagnostics of the crystalline nature of single organic nanocrystals by nonlinear microscopy," Phys. Rev. Lett. **92**, 207401 (2004).

1. Introduction

Second harmonic generation (SHG) in random materials was already considered in the early days of nonlinear optics as a way to achieve a pseudo-phase matching mechanism between the fundamental (pumping) wave and the second harmonic generated wave [1, 2]. Recently, this effect regained attention when in a difference frequency generation experiment in micro-crystals of ZnSe it was observed that a weak nonlinear generation became more efficient as the size of the micro-crystals approached one coherence length [3]. In contrast to what was expected from a periodically ordered material, SHG in ZnSe micro-crystals did not show a maximum, but as the average size of the domain was made larger than one coherence length, the generation did not decrease but remained constant instead, a behavior that was later attributed to the randomness in the size of the domains [4]. Parallel to this observation, an increasing interest developed in Strontium-Barium Niobate (SBN), a material where the nonlinear ferroelectric domains, characterized by a needle-like shape, are distributed randomly with the needle axis parallel to the c-axis of the bulk single crystal of the material [5–7]. Up to date, it has been generally assumed that in this kind of structures, when the fundamental field propagates in a direction perpendicular to the domain axis, the generated second harmonic light is scattered in all directions on a plane that contains the incident beam. This picture has been supported by a theoretical model in which the physical origin of the uniform in-plane SHG is attributed to a homogeneous distribution of reciprocal space vectors in all directions perpendicular to the polar axis of the crystal [6, 7].

In this letter, we show for the first time that the in-plane SHG from SBN crystals is not as uniform as it has been reported up to date, and that actually, under certain conditions, can display an intense generation in the forward direction. In order to explain this observation, we applied a theoretical model that captures all the physics involved and show that the main features observed in our experiments can be understood by analyzing the scattering of light by a single nonlinear domain. Importantly, notice that, although the enhancement of light scattering in certain directions has been extensively studied in random optical materials [8], here, for the first time, we report on enhanced light scattering in a transparent optical system featuring a homogeneous index of refraction. As we show below, the lack of scattering in the linear regime, along with the nonlinear light generation occurring at random positions inside the considered system, make the physical origin of the observed process to be radically different from those found up to date in linear random optical structures. In particular, we demonstrate that the larger average size of the nonlinear domains considered in this work with respect to previous studies of SHG in SBN [5–7] is crucial to enable the observation of the reported enhancement of the SHG signal.

2. Experimental results

The experimental analysis presented here was carried out using a SBN crystal characterized by a spontaneously grown random distribution of needle-like domains [5]. The domain structure is made visible by chemically etching in HF 48%. Since the acid etches faster the domains in one orientation than in the other, the polarization structure can be observed by scanning

#128859 - $15.00 USD Received 24 May 2010; revised 10 Jun 2010; accepted 12 Jun 2010; published 16 Jun 2010

electron micrographs (SEM) as differences in the surface relief. One of the SEM images taken during our experiments is displayed in Fig. 1(a). From inspection of several of these images, we determined an average domain size in the direction perpendicular to the axis of the needle (c-axis) of approximately 13 μm. In addition, from these images, we also observed that some of the nonlinear domains have circular section, while there are others which section resembles more that of a square with rounded corners. These square shapes appear to be all oriented in the same direction, following the cubic symmetry of the SBN crystal.

Figures 1(b) and 1(c) show the results of SHG experiments in which the SBN sample is pumped by a fundamental beam (consisting of a 1KHz train of 150 fs pulses tuned at λ_1=1200 nm) propagating along a direction parallel and perpendicular, respectively, to the c-axis of the crystal. Figure 1(b) clearly displays the expected ring-shaped SHG at λ_2=600 nm. Note however, the appearance of another ring of weaker intensity inscribed in the larger one. This secondary ring is more clearly visualized in inset of Fig. 1(b), which shows the total intensity along one diameter of the ring as measured by moving a detector in a plane perpendicular to the incident beam.

On the other hand, as shown in Fig. 1(c), when the sample is pumped in the direction perpendicular to the c-axis, the SHG strongly peaks at a direction very close to that of the incoming beam; the observed SHG maximum intensity being more than 100 times brighter than the scattered background generation (to mimic an observation at infinity in this experimental measurement, the detector was moved horizontally along the focal plane of a 250 mm lens placed right behind the crystal). A photograph of the corresponding SHG is shown in the left inset of Fig. 1(c), where that intense spot of generation is clearly visible on top of the dimmer line produced by scattered second harmonic light. To confirm that the SHG in the forward direction is a result of the random distribution of domains in the bulk of the crystal and to rule out any surface effect, we measured the energy at the peak as a function of the thickness of the crystal. As expected for this class of random structures [3, 4], we observed a linear growth of the second harmonic peak intensity [see right inset of Fig. 1(c)]. The same linear growth, as shown here is observed when we measure the intensity at any point of the background scattered second harmonic light. We note that slight deviations from a linear growth versus thickness, as for instance when the thickness of the crystal is close to 3.2 mm, are seen in the right inset of Fig. 1(c). These could be explained from a residual surface contribution to the SHG in the forward direction. Such surface contribution may exhibit a nonlinear thickness dependence as in the Maker fringes [9]. The same surface contribution may explain why, as described below, the experimental measurement provides a narrower peak in the forward direction than the one predicted by our theory of SH scattering by single domains.

3. Theoretical results and discussion

To understand the physics of our observations, and given that, to our knowledge, neither the observed burst of SHG nor the appearance of the secondary ring discussed above can be explained in general using the model employed up to date to describe SHG in random materials [6, 7], we have applied the Green function formalism to this problem [10, 11]. Let us briefly describe this theoretical framework. We start by considering SHG from an arbitrarily-shaped single nonlinear volume V_{NL} surrounded with a linear material of the same refractive index (which takes values n_1 and n_2 at the fundamental and second harmonic frequencies, respectively. In all the calculations shown in this manuscript we assume n_1=2.2795 and n_2=2.3479, which correspond to the values for the refractive index of SBN at λ_1=1.2 μm and λ_2=0.6 μm, respectively). Assuming all the fields to be time harmonic, the second harmonic E-field, $\mathbf{E}^{(2\omega)}(\mathbf{r})$, can be expressed in

#128859 - $15.00 USD Received 24 May 2010; revised 10 Jun 2010; accepted 12 Jun 2010; published 16 Jun 2010

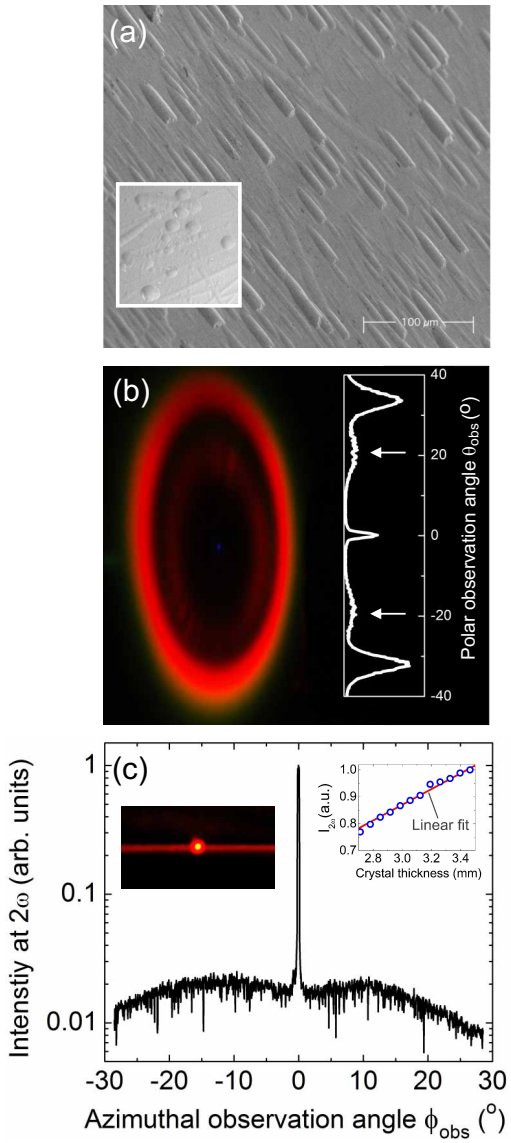

Fig. 1. (a) SEM picture of one of the SBN crystals used in the experiments. Main panel displays one of the surfaces parallel to the c-axis. The picture was taken after etching was carried out to make the nonlinear domains visible. The inset corresponds to an optical microscope picture taken from a surface perpendicular to the c-axis. (b) Picture of the second-harmonic light ring generated by the considered SBN crystal when the fundamental beam is propagating along the crystallographic c-axis. The spot in the center corresponds to a third harmonic generation in the direction of the incoming pump beam. Inset shows the experimental second harmonic intensity measured along one diameter of the generated light ring displayed in the main panel. The white arrows in the inset mark the angular locations of the secondary ring observed in the main figure. (c) Second-harmonic intensity scattered on a plane perpendicular to the c-axis of the SBN crystal as a function of the in-plane observation angle ϕ_{obs}. Left inset shows a picture taken from the light generation in this configuration. Right inset displays the second-harmonic peak power as a function of the thickness of the SBN crystal (blue circles). Red line in right inset corresponds to a linear fit through the data points that intersects with the origin.

#128859 - $15.00 USD Received 24 May 2010; revised 10 Jun 2010; accepted 12 Jun 2010; published 16 Jun 2010

terms of the corresponding electric dyadic Green's function $\widehat{G}(\mathbf{r},\mathbf{r}')$ as

$$\mathbf{E}^{(2\omega)}(\mathbf{r}) = \frac{(2\omega)^2}{c^2}\int_{V_{NL}} d\mathbf{r}'\,\widehat{G}(\mathbf{r},\mathbf{r}')\,\mathbf{P}^{(2\omega)}(\mathbf{r}') \tag{1}$$

where $\mathbf{P}^{(2\omega)}(\mathbf{r})$ stands for the induced nonlinear polarization at the second-harmonic frequency 2ω. The Cartesian components of $\mathbf{P}^{(2\omega)}(\mathbf{r})$ are defined by $P_i^{(2\omega)} = \varepsilon_0 \sum_{j,k} \chi_{ijk}^{(2)} E_j^{(\omega)} E_k^{(\omega)}$ (with $\chi_{ijk}^{(2)}$ being the corresponding second-order nonlinear susceptibility tensor, which is assumed to be compatible with the symmetry of the non-centrosymmetric ferroelectric phase of SBN; the indexes $\{i,j,k\}$ label the coordinates $\{x,y,z\}$, respectively, whereas $\mathbf{E}^{(\omega)}(\mathbf{r})$ represents the fundamental E-field). Notice also that the integral of Eq. (1) is performed over the nonlinear volume under study. For nonlinear volumes with simple external shapes (e.g., a cylinder or a rectangular parallelepiped) this integral can be performed analytically; otherwise it can be computed numerically.

Since, as mentioned, in order to reproduce the optical response of the experimental sample, we assume no refractive index difference between the nonlinear domain and the surrounding linear medium, $\widehat{G}(\mathbf{r},\mathbf{r}')$ can be obtained from the scalar Green's function of a three-dimensional homogeneous medium [12]. In addition, as we are interested in the far-field response, we can use the asymptotic expansion of $\widehat{G}(\mathbf{r},\mathbf{r}')$ in the limit $|\mathbf{r}| >> |\mathbf{r}'|$. Thus, if we assume a form for the fundamental E-field given by $\mathbf{E}^{(\omega)}(\mathbf{r}) = E_0^{(\omega)} \exp(i\mathbf{k}^{(\omega)}\mathbf{r})\,\mathbf{u}_E$ (where $\mathbf{u}_E$ is a unitary vector defining the polarization of the fundamental E-field, $E_0^{(\omega)}$ stands for the corresponding E-field amplitude, and $|\mathbf{k}^{(\omega)}| = \omega n_1/c$), Eq. (1) can be recast as

$$\mathbf{E}^{(2\omega)}(\mathbf{r}) = \frac{(2\omega)^2}{c^2}\left[E_0^{(\omega)}\right]^2 \frac{\exp(i\,|\mathbf{k}^{(2\omega)}|r_{obs})}{4\pi r_{obs}}\,\widehat{I}_{\Delta\mathbf{k}}(\phi_{obs},\theta_{obs})\,\mathbf{p}^{(2\omega)} \tag{2}$$

Here r_{obs} denotes the distance from the center of the considered nonlinear volume to the observation point, while ϕ_{obs} and θ_{obs} are the azimuthal and polar angles, respectively, defining the observation direction. The matrix $\widehat{I}_{\Delta\mathbf{k}}$ is defined as $\widehat{I}_{\Delta\mathbf{k}}(\phi_{obs},\theta_{obs}) = [\int_{V_{NL}} d\mathbf{r}' \exp(-i\Delta\mathbf{k}\mathbf{r}')] \times \widehat{M}(\phi_{obs},\theta_{obs})$, where $\Delta\mathbf{k} = |\mathbf{k}^{(2\omega)}|\mathbf{u}_r - 2\mathbf{k}^{(\omega)}$ ($\mathbf{u}_r$ denotes a unit vector pointing along the observation direction and $|\mathbf{k}^{(2\omega)}| = 2\omega n_2/c$). Notice that this $\Delta\mathbf{k}$ governs the phase-matching between the fundamental and second-harmonic fields propagating inside the considered nonlinear volume. On the other hand, the matrix $\widehat{M}$ is defined as $\widehat{M}(\phi_{obs},\theta_{obs}) = \widehat{I} - \mathbf{u}_r \otimes \mathbf{u}_r$ (the operator '$\otimes$' denotes a tensor product). Finally, $\mathbf{p}^{(2\omega)} = 2\,\widehat{d} \otimes \mathbf{u}_E \otimes \mathbf{u}_E$, where $\widehat{d}$ represents the contracted second-order nonlinear coefficient whose components are obtained from the tensor components $\chi_{ijk}^{(2)}$ in the usual manner [13]. Once $\mathbf{E}^{(2\omega)}(\mathbf{r})$ has been computed from Eq. (2), the far-field intensity distribution at 2ω, $I^{(2\omega)}(\mathbf{r})$, can be obtained simply by using the fact that $I^{(2\omega)}(\mathbf{r}) = (1/2)(c\varepsilon_0 n_2)|\mathbf{E}^{(2\omega)}(\mathbf{r})|^2$.

Now, we turn to the case in which the nonlinear volume V_{NL} is a cylinder of diameter d_c and height h [see Fig. 2(a)]. The effect of having a 3D parallelepiped with the same height h but different cross section, such as a square with rounded corners, will be discussed later. After some algebra, from Eq. (2) one can show that the angular second-harmonic intensity distribution emitted by the cylinder can be written analytically as

$$I^{(2\omega)}(\mathbf{r}) = \left(\frac{2\omega^2|\mathbf{k}^{(2\omega)}|^2}{\varepsilon_0 c^3\, n_2\, n_1^2}\right)\left(\frac{d_c^4 h^2}{r_{obs}^2}\right) d_{eff}^2\,[I^{(\omega)}]^2\,\mathrm{sinc}^2\left[\frac{\Delta k_z(\phi_{obs},\theta_{obs})h}{2}\right]\left\{\frac{J_1\left[\Delta k_{\|}(\phi_{obs},\theta_{obs})r_c\right]}{\Delta k_{\|}(\phi_{obs},\theta_{obs})r_c}\right\}^2 \tag{3}$$

where $I^{(\omega)}$ is the intensity of the fundamental E-field incident onto the sample, $I^{(\omega)} = (1/2)(c\varepsilon_0 n_1)|E_0^{(\omega)}|^2$. d_{eff} stands for the corresponding effective second-order nonlinear coe-

#128859 - $15.00 USD Received 24 May 2010; revised 10 Jun 2010; accepted 12 Jun 2010; published 16 Jun 2010

fficient. The function $\Delta k_z(\phi_{obs},\theta_{obs})$ denotes the projection of the phase-matching wavevector $\Delta\mathbf{k}$ onto the z axis, whereas $\Delta k_{\|}(\phi_{obs},\theta_{obs})$ stands for the magnitude of the projection of $\Delta\mathbf{k}$ onto the xy plane $\Delta\mathbf{k}_{\|}=|\Delta\mathbf{k}_{\|}|$. Finally, J_1 is the first-order Bessel function.

Notice that, in contrast with the theoretical model employed up to date for the analysis of second-harmonic generation from random optical materials (as mentioned above, based on considering a homogeneous distribution of vectors in the reciprocal space [14, 15]), in this work we apply a theoretical approach consisting in the analysis of the problem in real space. As we show below, this approach, based on Eq. (3), allows us to explain the physical origin of all the different features observed in our experiments in terms of the scattering of a single nonlinear volume.

Thus, the physical origin of the observed maximum of second-harmonic intensity in the xy plane shown in Fig. 1(c) emerges when looking at the conditions that maximize the expression for $I^{(2\omega)}(\mathbf{r})$ given in Eq. (3). Specifically, noticing that for $\theta_{obs}=\pi/2$ [see definition of polar and azimuthal angles in schematics of Figs. 2(a) and 2(b)], $\Delta k_z=0$ and $\Delta k_{\|}=\sqrt{n_2^2-n_1^2-2\,n_2\,n_1\cos(2\phi_{obs})}$, it is straightforward to deduce that $I^{(2\omega)}(\mathbf{r})$ peaks at $\phi_{obs}=0$. In fact, since one can show that this value of ϕ_{obs} corresponds to $\Delta k_y=0$, it is also clear that it is precisely the phase-matching in the direction perpendicular to the propagation direction (y-axis in the considered configuration) the main mechanism behind the appearance of the observed dramatic increase of SHG. We note that in the case of illumination perpendicular to the c-axis, the above-discussed enhancement of SHG signal is invariant with respect to the in-plane rotation of the reference frame (i.e., for the considered cylindrically-shaped domain, the SHG enhancement is always found in the forward direction with respect to the fundamental beam). Thus, without any loss of generality, in our calculations we have assumed the x-axis to be parallel to the direction of propagation of the fundamental beam, whereas the y-axis is defined along the direction perpendicular to both the propagation direction and the c-axis.

The result of this unusual phase matching in the direction perpendicular to the propagation direction is illustrated in Fig. 2(c), which shows the theoretical second-harmonic intensity emission pattern corresponding to a cylinder defined by d_c=13μm and h =26μm, computed for the case in which the fundamental beam propagates along the x-axis. Importantly, since for this configuration the minimum value for $\Delta k_{\|}$ is different from zero, the efficiency of generation oscillates with the radius of the cylinder, as shown in the inset of Fig. 2(c). A relative maximum is seen at $d_c\approx$13μm, which, remarkably, coincides with the experimentally determined average size of the domains. In addition, by analyzing numerically different 3D external shapes of the nonlinear volume V_{NL}, we have found that the above described phase-matching, responsible for the observed dramatic increase of SHG, seems to be rather independent of the shape of the domain. In particular, Fig. 2(e) renders the computed results for the case of a nonlinear parallelepiped of height h =26μm and whose cross section is a square with rounded corners (which, as mentioned, resembles some of the domains observed in the actual SBN crystal used in our experiments). The cross section area of this rounded parallelepiped is set to be equal to the cross section area of the cylinder considered in Fig. 2(c). Notice that the peak of SHG that can be observed in Fig. 2(e) at $\phi_{obs}=0$ is about two orders of magnitude larger than the value defined by the plateaus surrounding this maximum, which agrees with the relative height of the maximum of $I^{(2\omega)}(\mathbf{r})$ with respect to the scattered background observed experimentally [see Fig. 1(c)].

Figures 2(d) and 2(f) display the theoretical angular distributions of $I^{(2\omega)}(\mathbf{r})$ computed for the case in which the nonlinear cylinder and the parallelepiped with rounded cross sections considered above are illuminated by a fundamental beam propagating along the c-axis. Remarkably, both panels show clearly that the far-field distribution of SHG from a finite single domain is very similar to that found experimentally in a random distribution of domains. The

#128859 - $15.00 USD Received 24 May 2010; revised 10 Jun 2010; accepted 12 Jun 2010; published 16 Jun 2010

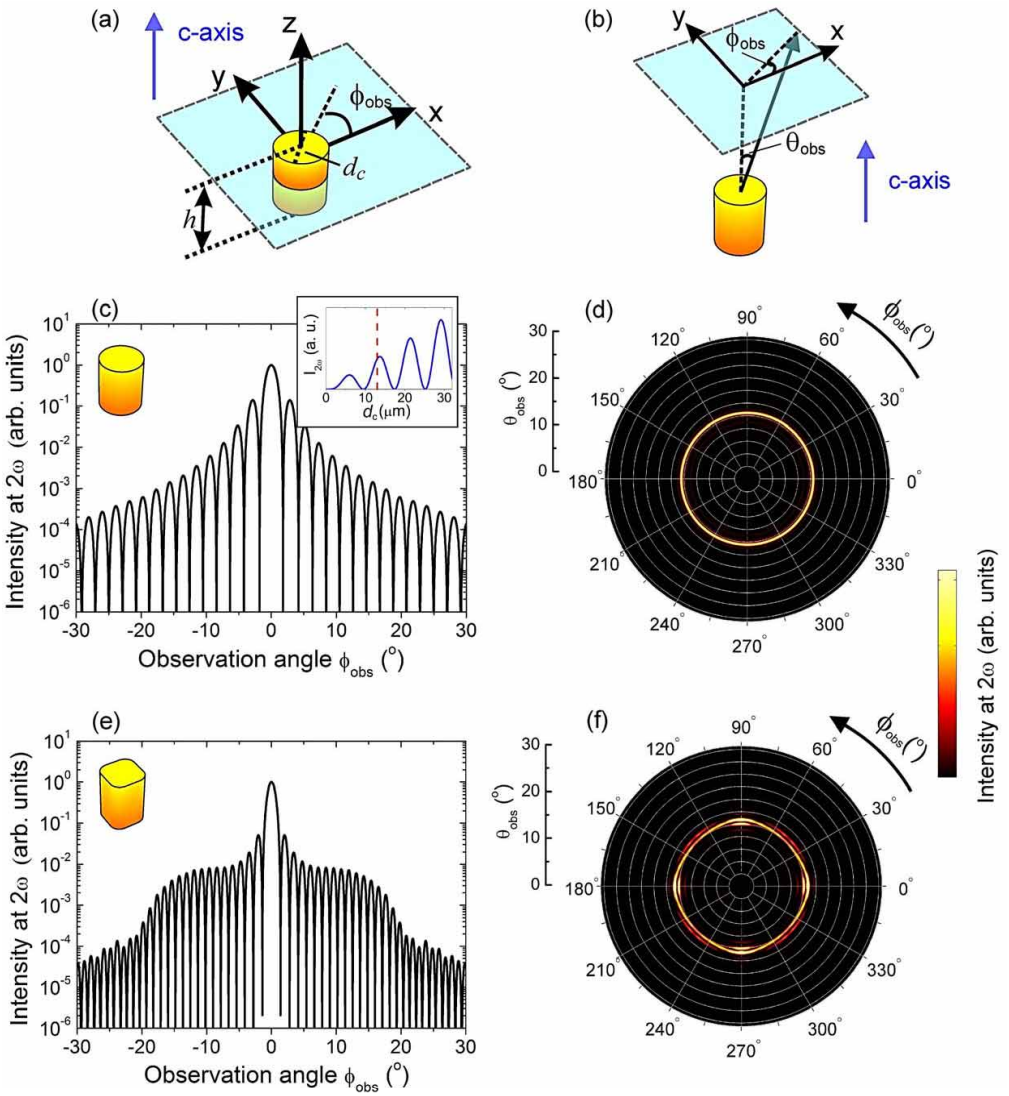

Fig. 2. (a),(b): Schematics of the two different configurations considered in the theoretical analysis. (c),(d): Computed far-field second-harmonic light distributions from a single nonlinear three-dimensional cylindrical volume (diameter d_c=13μm and height h=26μm) obtained for the case in which the fundamental beam is propagating in the direction perpendicular and parallel to the c-axis, respectively. (e),(f): As in (c) and (d), respectively, but for a nonlinear volume consisting of a three-dimensional parallelepiped with rounded edges.

#128859 - $15.00 USD Received 24 May 2010; revised 10 Jun 2010; accepted 12 Jun 2010; published 16 Jun 2010

physical origin of the ring-shaped emission from a single domain shown in Figs. 2(d) and 2(f), can also be unveiled by inspection of Eq. (3) as follows. In the configuration in which fundamental beam propagates in a direction parallel to the c-axis [see Fig. 2(b)], the projection of the phase-matching wavevector $\Delta\mathbf{k}$ along the c-axis is given by $\Delta k_z = (4\pi/\lambda_1)(n_2\cos\theta_{obs} - n_1)$. Noticing that the condition $\Delta k_z = 0$ maximizes $I^{(2\omega)}(\mathbf{r})$ for this configuration, we predict the existence of a ring-shaped emission with an angular aperture given by $\theta_a = \mathrm{acos}(n_1/n_2)$. This result is in agreement with the value of θ_a found in our experiments, as well as with the value for this magnitude reported in the literature [6, 7].

To investigate if the phase dependent formation of the main peak survives when we consider a random distribution of domains with different sizes and random positions in space, we turn now to the case of a structure formed by a random distribution of cylindrical domains whose transversal and longitudinal sizes are determined by a Gaussian random distribution. The mean value and the standard deviation of this random distribution are chosen to match those obtained from direct analysis of SEM images of the etched surfaces of our SBN crystal. Notice that, in general, the full description of the SBN crystal considered in this work, would require the inclusion of the anti-parallel nonlinear domains present in the interstices of the above described random distribution of cylindrical domains. However, since these interstitial volumes are irregular (i.e., the corresponding integrals can not be performed analytically), such calculations are a computational tour de force beyond our reach at the moment, which would preclude a direct comparison with the presented experimental results.

Figures 3(a) and 3(b) render the results obtained from our simulations assuming that the fundamental beam propagates along a direction parallel and perpendicular to the c-axis, respectively. The averaged results shown in both panels correspond to 400 different random distributions, each one formed by 240 nonlinear cylinders. The mean value of the diameter of the cylinder is $\langle d\rangle$ =13μm, while their average height is given by $\langle h\rangle = 2\langle d\rangle$. The standard deviation of the distribution is chosen to be σ=2.6μm. Figure 3(a) shows that, when the structure is illuminated along the c-axis, the far-field distribution of second-harmonic light is dominated by the appearance of a ring-shaped distribution of angles in which the SHG is more intense. As shown in left panel of Fig. 3(a), the aperture of far-field cone defined by this ring (θ_a=15.5°) is in excellent agreement wih the one obtained experimentally [θ_a=13.8°, see Fig. 1(c)]. Note that, in addition, our model does predict the existence of a secondary internal ring. It is important to notice that the peak of generation in the forward direction predicted by the single domain model survives, as shown in Fig. 3(b), when a random distribution of multiple domains is considered, confirming the experimental observation shown in Fig. 1(c). This peak of generation in the forward direction is more clearly visualized in the top inset of Fig. 3(b), in which the average second-harmonic intensity is plotted in linear scale as a function of the observation angle ϕ_{obs}. Furthermore, our simulations also confirm the linear growth of the second-harmonic intensity as a function of the number of nonlinear volumes included in our simulations [see bottom inset of Fig. 3(b)].

Finally, in order to analyze the influence that the shape of the nonlinear domains has on the angular distribution of second harmonic light described above, we have performed a set of simulations in which a number of the nonlinear cylindrical domains of the analyzed structure have been replaced by rectangular parallelepipeds whose corners have been rounded to emulate the domain shapes observed in the experimental samples. The results from these calculations are summarized in Fig. 3(c), in which different ratios of the number of parallelepipeds with rounded cross section over the total number of domains in the structure have been considered, ranging from 0 (no rounded parallelepipeds in the system) to 75% (i.e., 75% of all the domains forming the structure are parallelepipeds). As displayed in this figure, as the number of rounded parallelepipeds in the system increases, two side maxima develop at $\phi_{obs} = \pm 14°$. These two

#128859 - $15.00 USD Received 24 May 2010; revised 10 Jun 2010; accepted 12 Jun 2010; published 16 Jun 2010

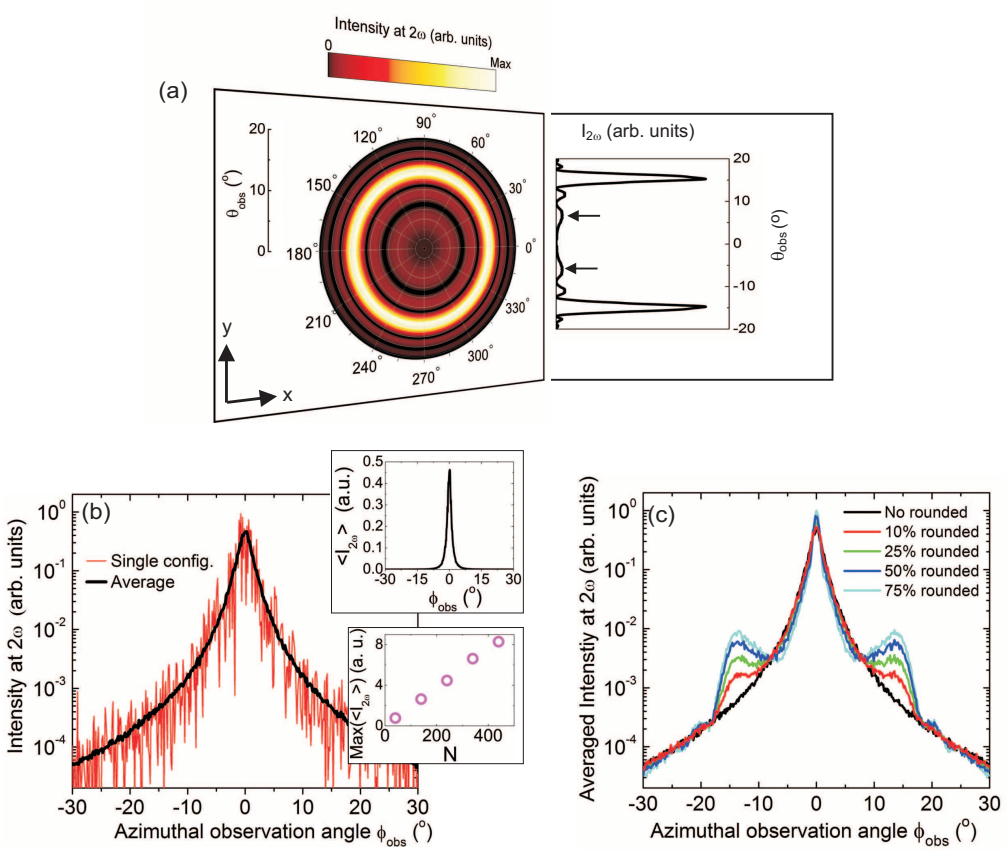

Fig. 3. (a) Simulated average far-field second-harmonic emission pattern for a random distribution of domains (see text for details on the distribution) computed for the configuration in which the fundamental beam propagates along the c-axis. Right inset: second harmonic intensity measured along one diameter of the generated light ring displayed in the main panel. Black arrows in this inset mark the locations of the inner right observed in the corresponding main figure. (b) Simulated SHG from the random distribution of nonlinear domains considered in (a), but now assuming that the fundamental beam propagates normally to the c-axis. Top inset: same as black line in main figure, but plotted now in linear scale. Bottom inset: calculated growth of second harmonic versus the number of cylinders. (c) Simulated second-harmonic intensity computed for random structures formed by a combination of nonlinear cylinders and rectangular parallelepipeds with rounded corners. Results for structures in which the percentage of nonlinear volumes that are parallelepipeds ranges from 0 (all the nonlinear volumes in the random structure are cylinders, see black line) to 75% (i.e., 25% of volumes in the random structure are cylinders, see cyan line) are shown.

#128859 - $15.00 USD Received 24 May 2010; revised 10 Jun 2010; accepted 12 Jun 2010; published 16 Jun 2010

peaks lead to a small increase of second harmonic light intensity as we move the observation angle away from the incident direction. The position of the two side maxima observed experimentally at $\phi_{obs} \approx \pm 5^{\circ}$ does not correspond to the prediction of the theory mostly because a correct effective observation at infinity is only achievable for small angles, for which the lens distortion is minimal.

4. Conclusions

To conclude, we have observed a non-homogeneous SHG from transparent nonlinear random structures. To explain the physical origin of these features of SHG in random configurations, we have applied a first-principles theoretical framework based on the Green function formalism. The results obtained from this approach fully agree with previous experimental observations of SHG from unpoled SBN crystals. This model conclusively shows that most of the observed characteristics of the nonlinear optical interaction in SBN are already present in the SHG from a single three-dimensional needle-shaped domain. We have demonstrated that such features rely on an unusual phase-matching within such single domain and that they survive when the collective contribution of many domains randomly distributed in space is considered. We believe the results reported in this letter open a broad range of opportunities to tailor the interaction of light with random distributions of nonlinear domains.

Acknowledgements

This work has been supported by Ministerio de Ciencia e Innovación (MICINN), under grants MAT2008-00910/NAN and CONSOLIDER NANOLIGHT grant CSD2007-00046. J.B.-A. acknowledges support by MICINN through Ramón y Cajal program, grant no. RyC-2009-05489.

#128859 - $15.00 USD Received 24 May 2010; revised 10 Jun 2010; accepted 12 Jun 2010; published 16 Jun 2010